MedCrave
Step into the World of Research

International Journal of Hydrology

Research Article

Open Access

CrossMark

3D flow of MHD tangent hyperbloic nanoliquid with the combined effect of soret and dufour effect past a heated convective stretching sheet

Abstract

Convective heat transport gives the remarkable behaviour in the many industrial procedure owing it mechanical behaviours of the system. A study has been obtained to analyse thermal radiative flow on unsteady MHD tangent hyperbolic nanoliquid near a stagnation point under viscous dissipation and chemical reaction. Also, thermal-diffusion and thermo-diffusion have been considered. The nonlinear PDE's are altered into a set of ODE's through suitable transformation and which are then numerically utilized. Further, numerical outputs for friction factor, Nusselt number and Sherwood are produced in table. Moreover, velocity distribution is increasing for a larger value of We and reduces for n. Moreover, similar behaviour is noted for temperature profile. A comparison with accessible outcomes for limited case is obtained with tremendous achievement.

Keyword: unsteady, nanofluid, heated convective, tangent hyper bolic fluid

Volume 6 Issue 4 - 2022

Farhan Ali,[1] Cherlacola Srinivas Reddy,[1] A Zaib,[1] M Faizan,[1] Khaled Al-Farhany,[2] Alphonsa Mathew[3]

[1]Department of Mathematical Sciences, Federal Urdu University of Arts, Sciences & Technology, Gulshan-e-Iqbal Karachi, Pakistan
[2]Department of Mechanical Engineering, university of Al-Qadisiyah, Al-Qadisiyah, Iraq
[3]St. Thomas college, Thrissur, India

Correspondence: Farhan Ali, Department of Mathematical Sciences, Federal Urdu University of Arts, Sciences & Technology, Gulshan-e-Iqbal Karachi, Pakistan,
Email farhanali.ali15@gmail.com

Received: March 15, 2022 | **Published:** July 05, 2022

Introduction

Recently, the enormous features have been utilized to increase the heat transport behaviours like changing geometry of flow and enhancing their thermal conductivity. Increasing challenges of more proficient heat transport liquid, there is require creating a new sort of fluid that are more influence in the form of heat transport phenomenon. The addition of nanoparticle in the ordinary fluid is one of the new science methods to boost heat transport increment. Most of the ordinary fluid like water, ethylene, glycol mixture have less heat transport rate. To enhance thermal conductivity with heat transport rate and it is essential to exploit the nanoparticles in the ordinary fluid. To envisage behaviour of nanoliquid several models have been presented in the literature. The novel idea was introduced Choi.[1] Later, the Buongiorno[2] has been attracted noteworthy attention owing to reasonable explanation of nanoparticles mechanism. Makinde and Aziz[3] numerically explored the viscous boundary layer nanoliquid near convective surface. Pal and Mondal[4] studied the MHD flow of non-isothermal nanofluid with convective condition near stagnation point. Turkyilmazoglu[5] reported an influence of the viscous fluid on the hydromagnetic nanoliquid flow of a heat and mass transmit due to a slip conditions. The generation/absorption on three dimensional Oldroyd-B nanoliquid near stretching surface with an effect of heat has considered by Khan et al.[6] In addition, Sisko nanoliquids past stretching sheet with the effect of heat transfer are presented via Khan et al.[7] The two constrain boundary conditions of nanoliquid due to a vertical surface has been deliberated by Kuznetsou and Nield.[8] Hayat et al.[9] developed the mixed convective flow visco-elastic nanofluids through a cylinder with heat source/sink. The MHD flow of nanomaterial with convective conditions has been created by Hayat et al.[10] A significant of nonlinear mechanics and utilising the effect of thermophoretic and Brownian movement are explained by Khan et al.[11,12]

The megnetohydrodynamic (MHD) are used in different areas of science and technology like molten metal and pumping station. The thermal stratification transient-free convective flows for nano liquid are investigated by Peddisetty.[13] The effect of heat sink-source with Burgers flow model under nanomaterial the due to stretched sheet considered by Khan and Khan.[14] The features of nanofluids for boosting the effectiveness of solar collectors are examined by Sheikh et al.[15] Khan et al.[16] conducted the effect of solar energy of MHD of Carreau nanofluid using the features of solar energy.

Now days, the demanding of the non-Newtonian fluids have been studied widely owing their significant applications in engineering, medicine and industries. There is non-linear correlation between shear stress and strain in this type of fluids. The study of non-Newtonian flow and the heat transport phenomena having shear effect. Cream, catch up and polymer solution are the few example of hyperbolic tangent fluid. This fluid model has sure benefit due to other than non-Newtonian fluid containing model formulation, simplicity of calculation and physical strength. Moreover, this flow model explains the blood flow very precisely.[17,18] Hayat et al.[19] examined MHD tangent hyperbolic nanoparticles over variable stretching surface. The EMHD unsteady hyperbolic tangent nano liquid with convective boundary condition has been observed by Mahdy and Hoshoudy.[20] Salahuddin et al.[21] noticed stagnation point and hyperbolic tangent nanomaterial due to a stretching cylinder. The numerically study of hyperbolic tangent nano liquid over sphere was considered by Gaffar et al.[22] The tangent hyperbolic due to stretching sheet and partial slip condition is ascertained by Ibrahim.[23] The influence of dual stratified on MHD tangent hyperbolic nano liquid due to permeable cylinder was conducted by Nagendramma et al.[24] Recently, Kumar et al.[25] examined three dimensional tangent hyperbolic fluid over bidirectional flow at convective boundary condition. More recently, Ramzan et al.[26] analysed the activation energy and Hall effect in a partially ionized tangent hyperbolic nano liquid under Cattaneo-Christive. The investigation shows that flows with nonlinear thermal radiation have not given much attention of many researchers because of wide ranging application. Such application contains design of furnace, gas turbines, glass production, nuclear plants, and space technologies. Cortell[27] presented nonlinear thermal radiative heat transfer near stretching

sheet. The three-dimensional Jeffrey nanofluid flow under nonlinear thermal radiation is investigated by Shehzad et al.[28] Pantokratoras and Fang[29] described Sakiadis flow and nonlinear Rosseland thermal radiative. Animasaun et al.[30] reported homogeneous/heterogeneous reactions within visco-elastic fluid flow under magnetic-field and nonlinear thermal radiative. MHD three-dimensional flow of nano liquid with velocity slip and nonlinear thermal radiative is explored by Hayat et al.[31] The 3D MHD nano liquid past shirking sheet with the combined result of thermal radiative with viscous dissipation are scrutinised by Nayak.[32] Ramzan et al.[33] explained 3D visco-elastic nano liquid with thermal radiative and mixed convection.

The aim of current of investigation is to communicate the 3-D flow MHD tangent hyperbolic nanofluid towards a stagnation point with heated convective condition. Study has been obtained under thermal radiation with chemical reaction, Soret and Dufour effects. Set systems of governing PDE's are reduced to the set of ODE using appropriate transformation. The set of ODE's are utilized through Bvp4C along shooting technique. Sketch for velocity, temperature and concentration as well as skin fraction, heat and mass have been displayed graphically and tabular form.

Rheological model of tangent hyperbolic

The Cauchy stress tensor is

$$\tau = \left[\mu_\infty + \left(\mu_\circ + \mu_\infty\right)\tanh\left(\Gamma\dot{\gamma}\right)^n\right]\dot{\gamma}, \tag{1}$$

where $\dot{\gamma}$ is stated as

$$\dot{\gamma} = \sqrt{\frac{1}{2}\sum_i\sum_j \dot{\gamma}_{ij}\dot{\gamma}_{ji}} = \frac{1}{2}\sqrt{\pi} \tag{2}$$

$$\pi = \frac{1}{2}tr\left(gradV + (gradV)^T\right)^2$$

Then tensor Eq. (1) become as

$$\tau = \mu_\circ\left[\left(\Gamma\dot{\gamma}\right)^n\right]\dot{\gamma} = \mu_\circ\left[1+\left(\Gamma\dot{\gamma}-1\right)^n\right]\dot{\gamma} = \mu_\circ\left[1+n\left(\Gamma\dot{\gamma}-1\right)\right]\dot{\gamma}. \tag{3}$$

Mathematical formulation

We ponder the unsteady 3D tangent hyperbolic nanofluid near stagnation point. The flow is persuaded along XY-plane (Z=0) through bidirectional stretched with streching velocities $U_w(x,t) = \frac{ax}{1-\chi t}$, $V_w(x,t) = \frac{bx}{1-\chi t}$, $U_e(x,t) = \frac{cx}{1-\chi t}$ along XY-direction, where a, b and c are constant. The flow occupied the region Z > 0. Seen in Figure 1 the geometrical representation of current investigation. A non-uniform magnetic field $B(t) = \frac{B_0}{\sqrt{1-\chi t}}$ is computed. Where B_0 is magnetic field strength.

$$\frac{\partial\bar{u}}{\partial x} + \frac{\partial\bar{v}}{\partial y} + \frac{\partial\bar{w}}{\partial z} = 0, \tag{4}$$

$$\frac{\partial\bar{u}}{\partial t} + \bar{u}\frac{\partial\bar{u}}{\partial x} + \bar{v}\frac{\partial\bar{u}}{\partial y} + \bar{w}\frac{\partial\bar{u}}{\partial z} = \bar{v}(1-n)\frac{\partial^2\bar{u}}{\partial z^2} + \sqrt{2}v n\Gamma\left(\frac{\partial\bar{u}}{\partial z}\right)\frac{\partial^2\bar{u}}{\partial z^2} + \sigma\frac{B_0^2(t)}{\rho}(U_e - u) + \frac{\partial U_e}{\partial t} + U_e\frac{\partial U_e}{\partial x}, \tag{5}$$

$$\frac{\partial\bar{v}}{\partial t} + \bar{u}\frac{\partial\bar{v}}{\partial x} + \bar{v}\frac{\partial\bar{v}}{\partial y} + \bar{w}\frac{\partial\bar{v}}{\partial z} = \nu(1-n)\frac{\partial^2\bar{v}}{\partial z^2} + \sqrt{2}v n\Gamma\left(\frac{\partial\bar{v}}{\partial z}\right)\frac{\partial^2\bar{v}}{\partial z^2} + \sigma\frac{B_0^2(t)}{\rho}(V_e - v) + \frac{\partial V_e}{\partial t} + U_e\frac{\partial V_e}{\partial x}, \tag{6}$$

$$\frac{\partial\bar{T}}{\partial t} + \bar{u}\frac{\partial\bar{T}}{\partial x} + \bar{v}\frac{\partial\bar{T}}{\partial y} + \bar{w}\frac{\partial\bar{T}}{\partial z} = \alpha_m\frac{\partial^2\bar{T}}{\partial z^2} + \frac{D_e k_T}{C_s C_p}\frac{\partial^2\bar{C}}{\partial z^2} + \tau\left(D_B\frac{\partial\bar{C}}{\partial z}\frac{\partial\bar{T}}{\partial z} + \frac{D_T}{T_\infty}\left(\frac{\partial\bar{T}}{\partial z}\right)^2\right) - \frac{1}{(\rho c)_f}\frac{\partial q_r}{\partial z} + \frac{\mu}{(\rho c)_f}\left[\left(\frac{\partial u}{\partial z}\right)^2 + \left(\frac{\partial v}{\partial z}\right)^2\right], \tag{7}$$

$$\frac{\partial\bar{C}}{\partial t} + \bar{u}\frac{\partial\bar{C}}{\partial x} + \bar{v}\frac{\partial\bar{C}}{\partial y} + \bar{w}\frac{\partial\bar{C}}{\partial z} = D_B\frac{\partial^2\bar{C}}{\partial z^2} + \frac{D_e k_T}{T_m}\frac{\partial^2\bar{T}}{\partial z^2} + \frac{D_T}{T_\infty}\left(\frac{\partial^2\bar{T}}{\partial z^2}\right) - \kappa_0(C_w - C_\infty), \tag{8}$$

$$u = u_w(x), v = v_w, w = w_0, T_w = T_\infty, C_w = C_\infty \text{ at z=0}$$
$$\text{u} \to 0, \text{v} \to 0, \text{T} \to T_\infty, C \to C_\infty \text{ at z} \to \infty \tag{9}$$

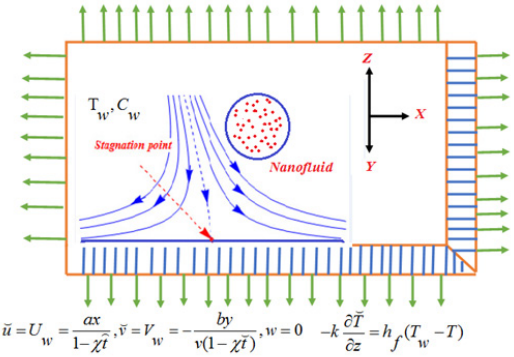

Figure 1 Model of the flow.

Considering the transformation

$$u = \frac{ax}{1-\chi t}f'(\eta), v = \frac{ay}{v(1-\chi t)}g'(\eta), w = -\sqrt{\frac{av}{1-\chi t}}\left[f(\eta)+g(\eta)\right] \tag{10}$$

$$\eta = \sqrt{\frac{a}{v(1-\chi t)}}z, \theta(\eta) = \frac{T-T_\infty}{T_w-T_\infty}, \ \phi(\eta) = \frac{C-C_\infty}{C_w-C_\infty}, h(t) = \frac{d}{\sqrt{1-\chi t}}.$$

$$(1-n)f'''+(f+g)f''-f'^2+nWef'''f''-\varepsilon\left(\frac{\eta}{2}f''+f'\right)+\varepsilon\lambda+\varepsilon^2+M(\varepsilon-f)=0 \tag{11}$$

$$(1-n)g'''+(f+g)g''-g'^2+nWeg'''g''-\varepsilon\left(\frac{\eta}{2}g''+g'\right)+\varepsilon\lambda+\lambda^2+M(\lambda-g)=0 \tag{12}$$

$$\theta''+R_d\left(1+(\theta_w-1)\theta\right)^2\left[3(\theta_w-1)\theta'^2+\left(1+(\theta_w-1)\theta\right)\theta''\right]+\Pr(f\theta'-\varepsilon\frac{\eta}{2}\theta')+ \tag{13}$$
$$+\Pr Ec\left(f'^2+g'^2\right)+\Pr D_f\phi''+\Pr Nb\theta'\phi'+\Pr Nt\theta'^2=0$$

$$\phi''+ScS_r\theta''+Sc\left(f-\frac{\eta}{2}\right)\varepsilon+\theta''\frac{Nt}{Nb}-Sc\kappa\phi=0 \tag{14}$$

With boundary conditions

$$f(0)=0, f'(0)=1, g'(0)=\alpha, g(0),$$
$$\theta'(0)=-\gamma\left(1-\theta(0)\right), \phi(0)=1, at\ y=0 \tag{15}$$
$$f'(\infty)\to\lambda, g'(\infty)\to 0, \theta(\infty)\to 0 as\ \ \text{y}\to\infty$$

The physical variables in the above expressions have been declared as follows

$We = \frac{\sqrt{2a}\Gamma U}{\sqrt{\upsilon}}$ (Weissenberg number)

$\varepsilon = \frac{a}{c}$ (Unsteadiness Parameters)

$D_f = \frac{D_e k_T(C_w - C_\infty)}{C_s C_p(T_f - T_\infty)\upsilon}$ (Dufour)

$Sr = \frac{D_e k_T(T_f - T_\infty)}{T_m\nu(C_w - C_\infty)}$ (Soret)

$Ec = \frac{U_w^2}{C_p(T_w - T_\infty)}$ (Eckert number)

$R_d = \frac{4\sigma^* T_\infty^3}{k^* k_f}$ (Radiation variable)

$N_b = \frac{\tau D_B}{\nu}\left(C_w - C_\infty\right)$ (Brownian motion)

$$N_t = \frac{\tau D_B}{\nu T_\infty}\left(T_w - T_\infty\right) \text{ (Thermophoresis)}$$

$$M = \frac{\sigma B_\circ^2}{\rho a} \text{ (Magnetic Parameter)}$$

$$\Pr = \frac{\nu}{\alpha_f} \text{ (Prandtl number)}$$

$$Sc = \frac{\nu}{D_B} \text{ (Scimdth number)}$$

The physical quantities

$$C_{fx} = \frac{\tau_{wx}}{\rho u_e^2}, \quad C_{fy} = \frac{\tau_{wy}}{\rho u_e^2}, \quad Nu_x = \frac{xq_w}{k(T_w - T_\infty)}, \quad Sh_x = \frac{xs_w}{D_b(C_w - C_\infty)}, \quad (16)$$

Where $\tau_{wx} = \mu\left(\partial u/\partial z\right)\Big|_{z=0}$ and $\tau_{wy} = \mu\left(\partial v/\partial z\right)\Big|_{z=0}$ are the shear stress along x and y directions, respectively, $q_w = -k\left(\partial T/\partial z\right)\Big|_{z=0}$ is heat flux, and $s_w = -D_b\left(\partial C/\partial z\right)\Big|_{z=0}$ is the mass flux.

Using similarity variables, we obtain

$$\left.\begin{aligned} C_{fx}\left[\mathrm{Re}_x\right]^{0.5} &= \left[(1-n)f''(0) + \frac{n}{2}We(f''(0))^2\right], \\ C_{fy}\left[\mathrm{Re}_x\right]^{0.5} &= \left[(1-n)g''(0) + \frac{n}{2}We(g''(0))^2\right], \\ \left[\mathrm{Re}_x\right]^{-1/2} Nu_x &= -\theta'(0), \quad \left[\mathrm{Re}_x\right]^{-1/2} Sh_x = -\phi'(0). \end{aligned}\right\} \quad (17)$$

Where $\mathrm{Re}_x = \frac{u_x(x)x}{\nu}$

Implemented Strategy

The highly nonlinear ODE's Eqs. (11) - (14) associated to boundary condition Eq. (15) are transmuted into first order with along Bvp4C-technique for diverse values of emerging parameters. For the purpose, we choose new variables

$$\left.\begin{aligned} z_1' &= z_2 && z_1(0) = 0, \\ z_2' &= z_3 && z_2(0) = 1, \\ z_3' &= \frac{z_2^2 + \varepsilon\left(\frac{\eta}{2}z_3 + z_2\right) - (z_1 + z_4)z_3 - \varepsilon\lambda - \lambda^2 - M(\varepsilon - z_1)}{\left[(1-n) + nWez_3\right]} && z_3(0) = l, \\ z_4' &= z_5 && z_4(0) = 0, \\ z_5' &= z_6 && z_5(0) = \alpha, \\ z_6' &= \frac{z_5^2 + \varepsilon\left(\frac{\eta}{2}z_6 + z_5\right) - (z_1 + z_4)z_6 - \varepsilon\lambda - \lambda^2 - M(\lambda - z_4)}{\left[(1-n) + nWez_6\right]} && z_6(0) = m, \\ z_7' &= z_8 && z_7(0) = n, \\ z_8' &= \frac{-1}{Rd\left(1 + (\theta_w - 1)z_7\right)^7}\begin{pmatrix} Rd\left(1 + (\theta_w - 1)z_7\right)^2\left(3(\theta_w - 1)z_8^2\right) \\ + \Pr\left(z_1 z_8 - \varepsilon\frac{\eta}{2}z_8\right) + \Pr Ec\left(z_1^2 + z_2^2\right) \\ + \Pr D_f z_{10}' + \Pr Nbz_8 z_{10} + \Pr Ntz_8^2 \end{pmatrix} && z_8(0) = -\gamma(1-n), \\ z_9' &= z_{10} && z_9(0) = 1, \\ z_{10}' &= Sc\kappa z_9 - ScSrz_8' - Sc\left(z_1 - \frac{\eta}{2}\right)\varepsilon - z_8'\frac{Nt}{Nb} && z_{10}(0) = o, \end{aligned}\right\}$$

The above defined set of first ODE's is utilized via Runge-Kutta method by assigning few missing variables *l*, m, n and o. The step has measured as $\Delta\eta$. The process is frequent until criterion is not converge of 10^{-6}.

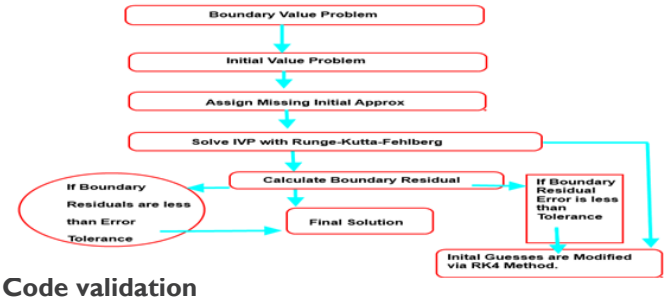

Code validation

To verify the precision of current calculated outcomes with previous available data, a evaluation has made between latest computed outcomes and existing literature in limiting case. Table.1 exhibits a comparing of the numeric outcomes for the skin fraction for the various estimation of $f''(0)$ for various estimation of the unsteady $\mathcal{E}$ variable when We = n = 0, published outcomes of Ali and Zaib[35] and Khan et al.[34] shown in Table 1. These outcomes are obtained in remarkable achievement.

Table 1 Comparing of $f''(0)$ for unsteady parameter ε with $n = We = \lambda = M = 0$

ε	Khan and Hamid[34]	Ali and Zaib[35]	Current result
0.8	-1.26148	-1.26121	-1.26069
1.2	-1.37785	-1.37763	-1.37771

Result and discussion

The physical variables for $f'(\eta)$, $\theta(\eta)$ and $\phi(\eta)$ profiles are displayed graphically Figure 2–19. These physical parameters are kept constant entire study with their value n=0.2, We=0.3, ε =0.1, M=0.4, λ =0.1, Rd=0.4, θ_w =0.4, Nb=0.3, Nt=0.3,Df=0.03,Sr=0.4,Pr=0.7, Sc=0.8, γ =0.02 and α =0.8. Table 2 show the numerically result of various value of emerging parameter. Enlarging the value of We and n accelerates the skin friction. While it is noted that rate of Nusselt and Sherwood fall down by increasing value of Rd and k.

Figure 2–4 are displayed to views the result of (n) on $f'(\eta)$, $g'(\eta)$, $\theta(\eta)$ and $\phi(\eta)$. From the Figure 2 dimensionless velocity and concentration was reduced for the increasing value of (n). Actually, higher value of n boosts to improved the pressure on the flow results reduction in velocity and concentration and increment in thickness of layer and solutal boundary layer. Figure 5–7 have revealed to view the unsteady parameter (ε) velocity $f'(\eta)$, $g'(\eta)$, temperature $\theta(\eta)$ and concentration of nanoparticle $\phi(\eta)$. An increasing behavior in the nanofluid velocity component and boundary layer thickness enhanced due to the larger value of unsteady parameter. Due to this reason, unsteady variable is directly relative to the stretching rate of nanofluid with x-direction. Because escalated the unsteady variable the stretching rate with x-axis increases causes to upsurges nanofluid. Similar, behavior is seen for thermal and nanoparticles concentration. Figure 8–10 displays the of (We) on $f'(\eta)$, $g'(\eta)$, $\theta(\eta)$ and $\phi(\eta)$. Figure 8 larger the value of We upsurge in momentum layer and velocity. It is a fact that We is a thermal relation time to increase more flow of fluid. From Figure 9 is plotted to view that temperature of nanofluid is augmented for the greater value of We. Physically, an enhanced in thermal relaxation process result the increased in fluid temperature. From Figure 10 is sketch to clear that concentration of nanoparticles is intensified for increment value of We. Figure 11–13 shows the $f'(\eta)$, $g'(\eta)$ $\theta(\eta)$ and $\phi(\eta)$ for the variation of A. It is noted that from Figure 11 when (λ >1), the flow made boundary layer structure, from the fact that the shear effect toward the stagnation section accelerated so the augmentation of the outer stream enhances results diminish

the thickness of the boundary layer causes larger magnitude of λ. When (λ<1). For λ=1 there is no boundary layer structure is noted for the reason that both free stream and stretching velocity are equal. Velocity filed $g'(\eta)$ increases with greater value of λ. From Figure 12 and Figure 13 show that both θ(η) and ϕ(η) increases due to rise in λ.

Table 2 Comparison of Skin fraction ($\mathrm{Re}_x^{1/2} C_{fx}$, $\mathrm{Re}_x^{1/2} C_{fy}$) Nusselt ($\mathrm{Re}_x^{-1/2} Nu_x$) and Sherwood number ($\mathrm{Re}_x^{-1/2} Sh_x$) for various of n, we, Rd, Sr, Df, k

n	We	ε	Rd	Sr	Df	K	$\mathrm{Re}_x^{1/2} C_{fx}$	$\mathrm{Re}_x^{1/2} C_{fy}$	$\mathrm{Re}_x^{-1/2} Nu_x$	$\mathrm{Re}_x^{-1/2} Sh_x$
0.1	0.1	0.1	0.1	0.1		0.1	1.0994	0.7033	0.2791	1.2285
0.3	0.5			0.4			1.2868	0.7893	0.2608	1.0964
0.5	1			0.7			1.474	0.8545	0.2554	1.018
		0.2	0.3			0.6	0.6748	0.4305	0.5207	1.7698
							0.7117	0.4505	0.4218	1.6704
							0.8174	0.5058	0.3115	1.603
		0.3	0.5			1.2	0.4172	0.223	0.7632	2.3029
							0.433	0.2676	0.6283	2.1581
							0.4758	0.2892	0.463	2.1014

Table 3 Nomenclature

λ	**Free stream velocity**	T_w	**Sheet surface(wall) temperature**
a	Constant	T_∞	Ambient temperature
b	Constant	u,v	Velocity component along x-axis and y-axis
R_d	Radiation Parameter	X	Coordinate along the sheet
D_B	Brownian diffusion coefficient	Y	Coordinate normal to the sheet
D_T	Thermophoresis diffusion coefficient	C	Nano particle volume friction
D_f	Dufour number	Cw	Nano particle volume friction at the sheet surface (wall)
M	Magnetic field Parameter	C_∞	Nano particle volume friction (ambient)
n	Power-law index	Greek symbol	
k	Thermal conductivity of base fluid	α	Thermal diffusivity of the base fluid
Sr	Soret number	ε	Unsteady parameter
Sc	Schmidt number	ρ_{nf}	Nanofluid density
Nb	Brownian motion parameter	δ	Fluid constant
Nt	Thermophoresis parameter	ϕ	Dimensionless nanoparticle volume friction
Nu	Nussel tnumber	θ	Dimensionless temperature
Nur	Reduced Nusseltnumber	η	Similarity variable
Pr	Prandlt number		Absolute viscosity of the base fluid
$q_w^{"}$	Wall heat flux	υ	Kinematic viscosity of the base fluid
$q_m^{"}$	Mass flux	ρ_f	Density of base fluid
Re_x	Local Reynolds number	ρ_p	Nanoparticle mass density
Sh	Sherwood number	$(pC)_f$	Heat capacity of fluid
Shr	Reduced Sherwood number	$(pC)_p$	Effective heat capacity of the nanoparticle material
T	Local fluid temperature	τ	$(pC)_p/(pC)_f$
T_f	Temperature of the hot fluid	Ψ	Stream function

A significant of Nt and Nb for temperature and concentration of nanoparicle are explored in Figure 14–17. From Figures. the θ(η) and ϕ(η) distribution is increased for increasing value of Nt. From Figure 16,17 shown that the Nb boosts the temperature and reduced the concentration of nanoparticle. A fluid particle intensifies with augmentation in Nb and more heat is formed to amplify the thermal layer thickness. While enlarging value of Nb reduces nanoparticle concentration. Physically, boost in the magnitude of Nb result to enhance the rate of diffusions of nanoparticles in the base fluid motion in irregular direction. So, motion of nanoparticles escalates in convey of heat and decline in concentration.

Figure 18 exhibits the effect of (Pr) on θ(η). Clearly from Figure 18 larger Pr fallout temperature profile whereas the fluid become more viscous. Consequently, fluid with a less viscosity obtained a leading temperature and greater viscosity produced the lesser temperature. So, by growing in Pr leads to thermal diffusivity which decline temperature of tangent hyperbolic fluid. The θ(η) for the variation

of Rd has been exhibited in Figure 19. It describes that increase in temperature leading function of Rd. Physically, higher the radiation parameter Rd heat is produced in working fluid that is the reason temperature gradient accelerates. Temperature profile for diverse values of Ec has been indicated in Figure 20. Fluid temperature escalates for larger value of Ec. In this regard the increment in Eckert number Ec results increase in internal source of energy and that is the reason fluid temperature rise.

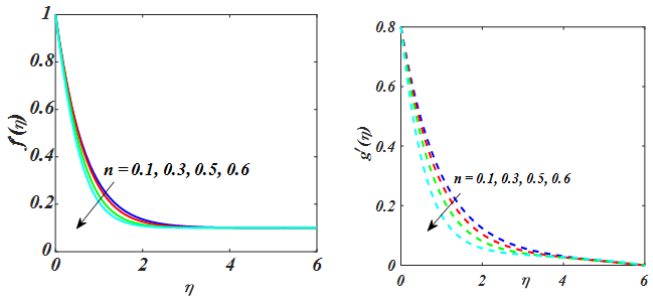

Figure 2 f' and g' for value of n.

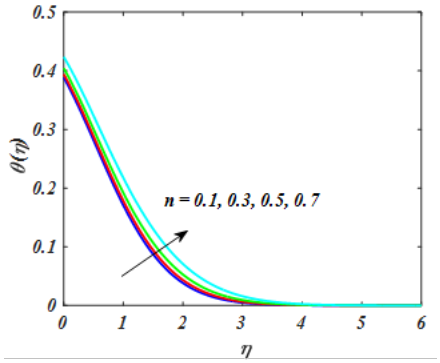

Figure 3 θ for value of n.

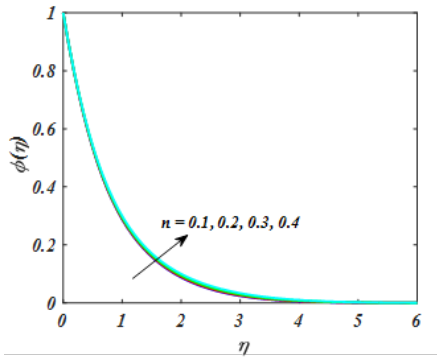

Figure 4 ϕ for value of n.

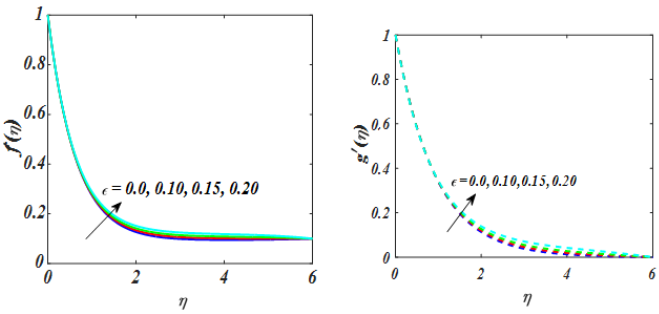

Figure 5 f' and g' for value of ε .

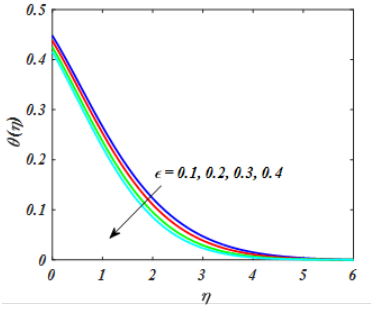

Figure 6 θ for value of ε .

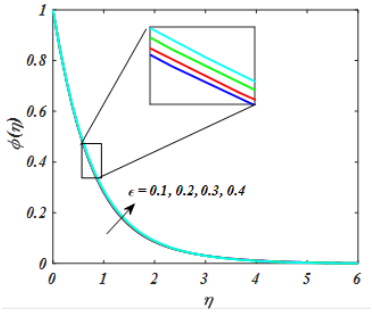

Figure 7 ϕ for value of ε .

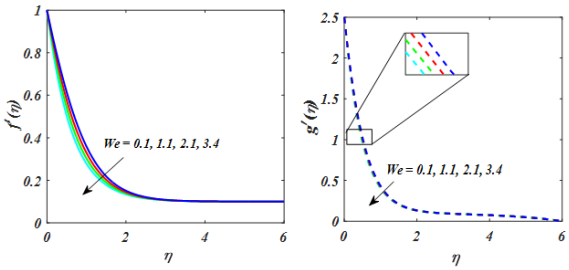

Figure 8 f' and g' for value of We.

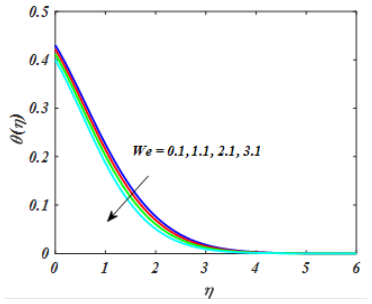

Figure 9 θ for value of We.

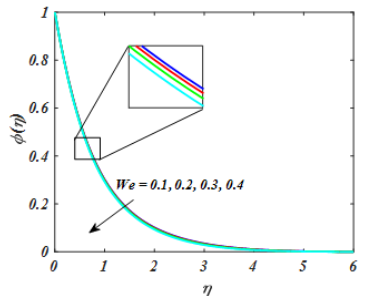

Figure 10 ϕ for value of We.

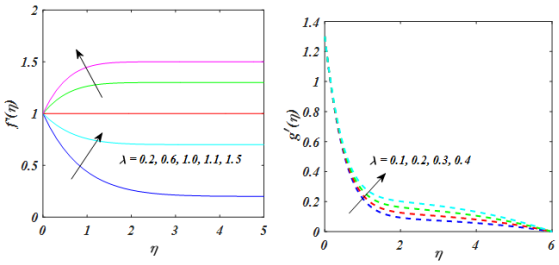

Figure 11 f' and g' for value of λ.

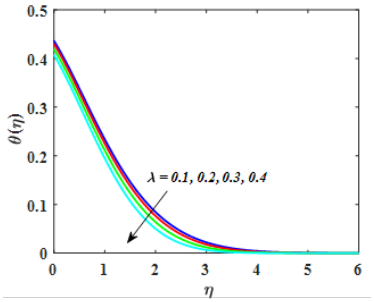

Figure 12 θ for value of λ.

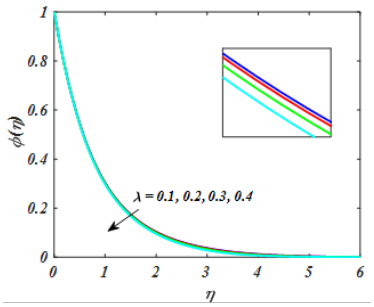

Figure 13 ϕ for value of λ.

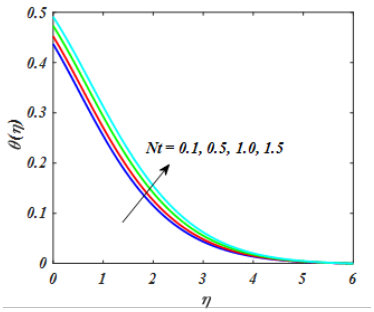

Figure 14 θ for value of Nt.

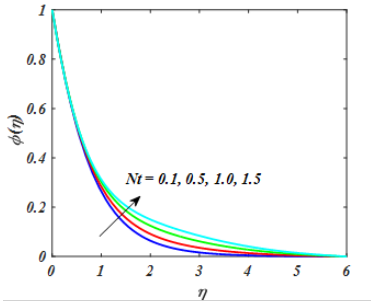

Figure 15 ϕ for value of Nt.

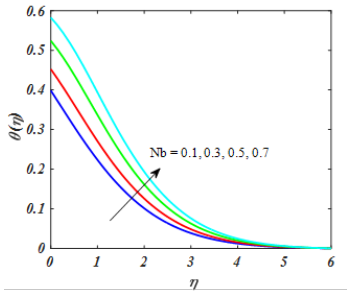

Figure 16 θ for value of Nb.

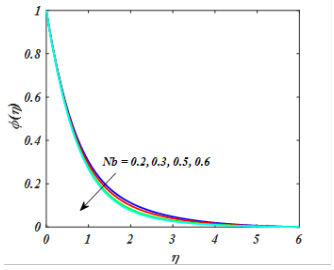

Figure 17 ϕ for value of Nb .

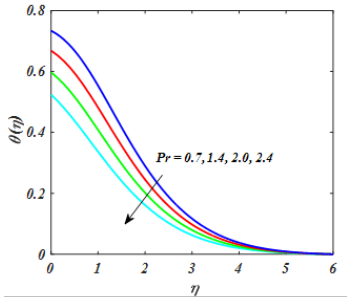

Figure 18 θ for value of Pr.

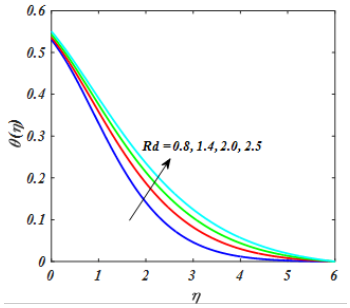

Figure 19 θ for value of Rd.

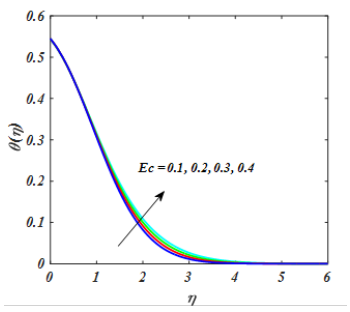

Figure 20 θ for value of Ec.

Citation: Ali F, Reddy CS, Zaib A, et al. 3D flow of MHD tangent hyperbloic nanoliquid with the combined effect of soret and dufour effect past a heated convective stretching sheet. *Int J Hydro.* 2022;6(4):108–116. DOI: 10.15406/ijh.2022.06.00315

Figure 21,22 depicted the effect of Sc and k on nanofluid concentration. It is notable that an augment k and Sc has a trend to decline the nanofluid concentration.

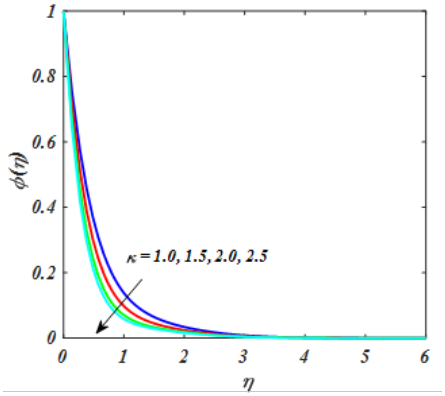

Figure 21 ϕ for value of K.

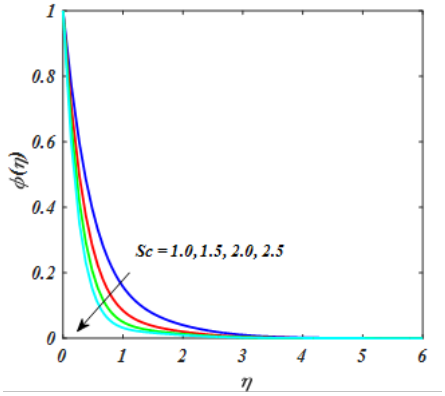

Figure 22 ϕ for value of Sc.

The effect of n and We on C_{fx}, C_{fy} wass illustrated in Figure 23,24. It shows that the C_{fx}, C_{fy} upsurges in favour of the different value of n and We. The persuade of Rd and Df on Nu_x is revealed in Figure 25. It is clear from the Fig. that the Nu_x depreciates for larger value of Rd and Df. The impact of k and Sr on Sh_x was seen in Figure 26. Sh_x reduced for greater value of k and Sr. Figure 27 shows the plot of stream line pattern for We and n.

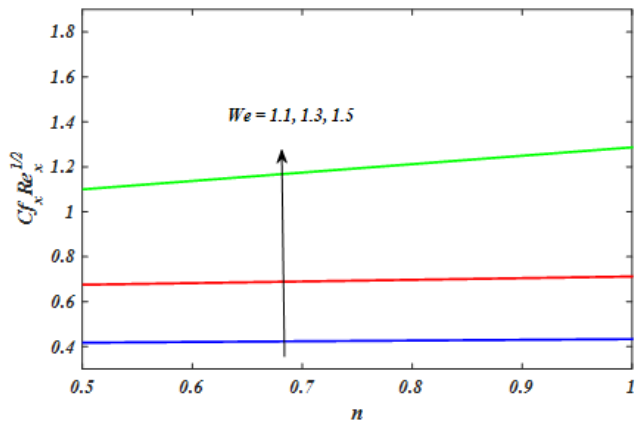

Figure 23 the impact of n and We on C_{fx}.

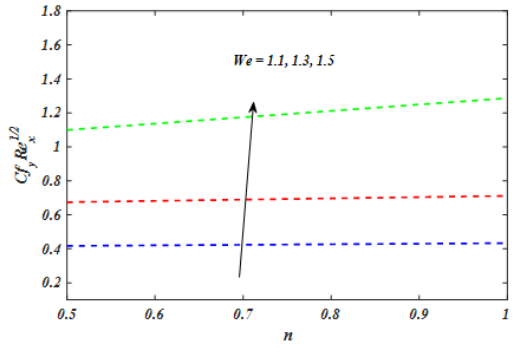

Figure 24 the impact of n and We on C_{fy}.

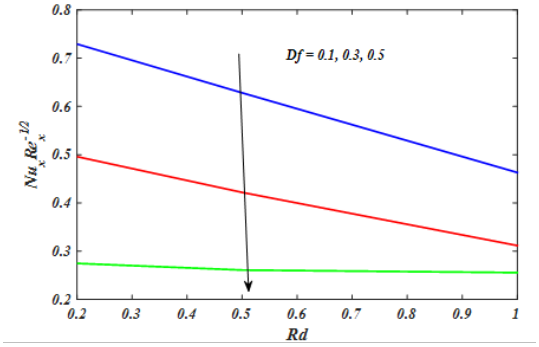

Figure 25 the impact of Df and Rd on Nu_x.

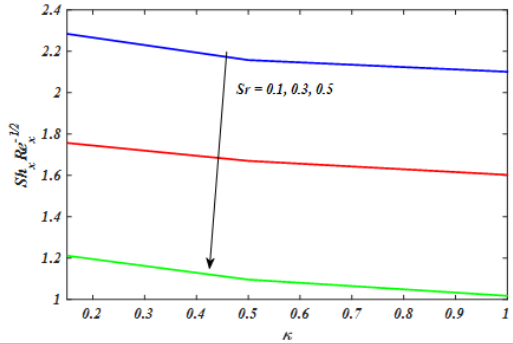

Figure 26 the impact of n and We on Sh_x.

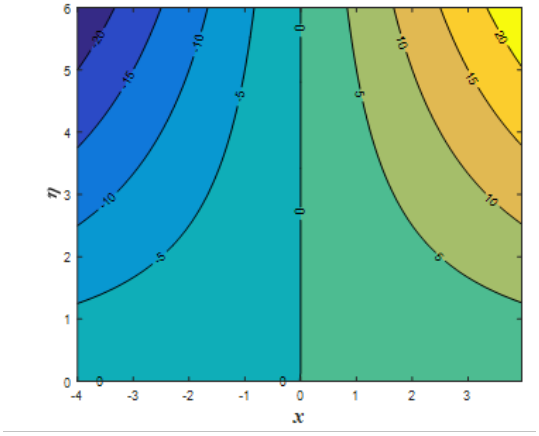

Figure 27 Stream line Pattern for n and We.

Final remarks

The current paper explored the 3D effect of tangent hyperbolic MHD flow in presence of Soret and Duofer. The major results of current analsis are given below.

I. Increase value of n and We due to increase in temperature.

II. Unsteady parameter ε increases both the velocities f' *and* g'.

III. Both temperature and concentration field are enhancing behaviour for Nt.

IV. Eckert number and Radiation parameter were increased while converse effect is noted in Pr.

V. Skin friction C_{fx}, C_{fy} enhances with enhancing value of n, We.

Acknowledgments

None.

Conflicts of interest

We have no conflict of interest.

References

1. SUS Choi. Enhancing thermal conductivity of fluids with nanoparticles, in Proceedings of the 1995 ASME International Mechanical Engineering Congress and Exposition. *San Francisco*. 1995;231:99–103.
2. J Buongiorno. Convective transport in nanofluids." *ASME J Heat Transf*. 2006;128:240–250.
3. OD Makinde, A Aziz. Boundary layer flow of a nanofluid past a stretching sheet with a convective boundary condition. *Int J Therm Sci*. 2011;50:326.
4. D Pal, H Mondal. Effects of Soret Dufour, chemical reaction and thermal radiation on MHD non-Darcy unsteady mixed convective heat and mass transfer over a stretching sheet, Commun. *Nonlinear Sci Numer Simul*. 2011;16:1942.
5. M Turkyilmazoglu. Exact analytical solutions for heat and mass transfer of MHD slip flow in nanofluids. *Chem Eng Sci*. 2012;84:182.
6. WA Khan, M Khan, R Malik. Three-Dimensional Flow of an Oldroyd-B Nanofluid towards Stretching Surface with Heat Generation/Absorption. *PLoS ONE*. 2014;9(8):e10510.
7. M Khan, R Malik, A Munir, et al. Flow and Heat Transfer to Sisko Nanofluid over a Nonlinear Stretching Sheet. *PLoS ONE*. 2015;10:e0125683.
8. AV Kuznetsou, DA Nield. Natural convective boundary-layer flow of a nanofluid past a vertical plate: A revised model. *Int J Therm Sci*. 2014;77:126.
9. T Hayat, M Waqas, SA Shehzad. Et al. Mixed convection flow of viscoelastic nanofluid by a cylinder with variable thermal conductivity and heat source/sink. *Int J Numer Methods Heat Fluid Flow*. 2014;26:214.
10. T Hayat, M Imtiaz, A Alsaedi. MHD 3D flow of nanofluid in presence of convective conditions. *J Magn Magn Mater*. 2015;395:294.
11. M Khan, WA Khan. Forced convection analysis for generalized Burgers nanofluid flow over a stretching sheet. *AIP Adv*. 2015;5:107138.
12. M Khan, WA Khan. MHD boundary layer flow of a power-law nanofluid with new mass flux condition. *AIP*. 2016;6
13. NC PEDDISETTY. Effects of thermal stratification on transient free convective flow of a nanofluid past a vertical plate. *Pramana - J Phys*. 2016;87:62.
14. M Khan, WA Khan. Steady flow of Burgers' nanofluid over a stretching surface with heat generation/absorption. *J Braz Soc Mech Sci Eng*. 2016;38:2359–2367.
15. NA Sheikh, F Ali, I Khan. On the applications of nanofluids to enhance the performance of solar collectors: A comparative analysis of Atangana-Baleanu and Caputo-Fabrizio fractional models. *Eur Phys J Plus*. 2017;132:540.
16. M Khan, M Iran, WA Khan. Numerical assessment of solar energy aspects on 3D magneto-Carreau nanofluid: A revised proposed relation. *Int J Hydrogen Energy*. 2017;42:22054.
17. VR Prasad, SA Gaffar, OA Beg. Free convection flow and heat transfer of tangent hyperbolic past a vertical porous plate with partial slip. *J App Fluid Mech*. 2016;9:1667–1678.
18. M Khan, A Hussain, MY Malik, et al. Boundary layer flow of MHD tangent hyperbolic nanofluid over a stretching sheet: A numerical investigation. *Results in Physics*. 2017;7:2837–2844.
19. T Hayat, M Waqas, A Alsaedi, et al. Magnetohydrodynamic (MHD) stretched flow of tangent hyperbolic nanoliquid with variable thickness. *Journal of Molecular Liquids*. 2017;229:178–184.
20. A Mahdy, G Hoshoudy. EMHD time-dependant tangent hyperbolic nanofluid flow by a convective heated Riga plate with chemical reaction. Proceedings of the Institution of Mechanical Engineers. *Part E: Journal of Process Mechanical Engineering*. 2019;233:776–786.
21. T Salahuddin, MY Malik, A Hussain, et al. Analysis of tangent hyperbolic nanofluid impinging on a stretching cylinder near the stagnation point. *Res Phys*. 2017;7:426–434.
22. SA Gaffar, VR Prasad, OA Bég. Numerical study of flow and heat transfer of non-Newtonian Tangent Hyperbolic fluid from a sphere with Biot number effects. *Alexandria Engineering Journal*. 2015;54:829–841.
23. W Ibrahim. Magnetohydrodynamics (MHD) flow of a tangent hyperbolic fluid with nanoparticles past a stretching sheet with second order slip and convective boundary condition. *Res Phys*. 2017;7:3723–3731.
24. V Nagendramma, A Leelarathnam, CSK Raju, et al. Doubly stratified MHD tangent hyperbolic nanofluid flow due to permeable stretched cylinder. *Res Phys*. 2018;9:23–32.
25. KG Kumar, S Manjunatha, BJ Gireesha, et al. Numerical illustrations of 3D tangent hyperbolic liquid flow past a bidirectional moving sheet with convective heat transfer at the boundary. *Heat Trans*. 2019;48:1899–1912.
26. M Ramzan, H Gul, JD Chung. Significance of Hall effect and Ion slip in a threedimensional bioconvective Tangent hyperbolic nanofluid flow subject to Arrhenius activation energy. *Sci Rep*. 2020;10:18342.
27. R Cortell. Fluid flow and radiative nonlinear heat transfer over stretching sheet. *J King Saud Univ Sci*. 2013;26:161–167.
28. SA Shehzad, T Hayat, A Alsaedi, et al. Nonlinear thermal radiation in three-dimensional flow of Jeffrey nanofluid: a model for solar energy. *Appl Math Comput*. 2014;248:273–286.
29. A Pantokratoras, T Fang. Sakiadis flow with nonlinear Rosseland thermal radiation. *Phys Scripta*. 2013;87:015703.
30. IL Animasaun, CSK Raju, N Sandeep. Unequal diffusivities case of homogeneous heterogeneous reactions within viscoelastic fluid flow in the presence of induced magnetic-field and nonlinear thermal radiation. *Alex Eng J*. 2016.
31. T Hayat, M Imtiaz, A Alsaedi, et al. MHD three-dimensional flow of nanofluid with velocity slip and nonlinear thermal radiation. *J Mag Mag Mater*. 2015;396:31–37.
32. MK Nayak. MHD 3D flow and heat transfer analysis of nanofluid by shrinking surface inspired by thermal radiation and viscousdissipation. *International Journal of Mechanical Sciences*. 2017;03014.

33. M Ramzan, M Bilal, U Farooq, et al. Mixed convective radiative flow of second grade nanofluid with convective boundary conditions: An optimal solution. *Res Phys*. 2016;6:796–804.

34. M Khan, A Hamid. Influence of non-linear thermal radiation on 2D unsteady flow of a Williamson fluid with heat source/sink. *Res Phys*. 2017;7:3968–3975.

35. F Ali, A Zaib. Unsteady flow of an Eyring-Powell nanofluid near stagnation point past a convectively heated stretching sheet. *Arab J Basic App Scis*. 2019;26:215–224.